Structure and Rotations of the Hoyle State

Evgeny Epelbaum,[1] Hermann Krebs,[1] Timo A. Lähde,[2] Dean Lee,[4] and Ulf-G. Meißner[5,2,3]

[1]*Institut für Theoretische Physik II, Ruhr-Universität Bochum, D-44870 Bochum, Germany*
[2]*Institut für Kernphysik, Institute for Advanced Simulation, Jülich Center for Hadron Physics,*
Forschungszentrum Jülich, D-52425 Jülich, Germany
[3]*JARA—High Performance Computing, Forschungszentrum Jülich, D-52425 Jülich, Germany*
[4]*Department of Physics, North Carolina State University, Raleigh, North Carolina 27695, USA*
[5]*Helmholtz-Institut für Strahlen- und Kernphysik and Bethe Center for Theoretical Physics,*
Universität Bonn, D-53115 Bonn, Germany
(Received 14 August 2012; published 17 December 2012)

The excited state of the ^{12}C nucleus known as the "Hoyle state" constitutes one of the most interesting, difficult, and timely challenges in nuclear physics, as it plays a key role in the production of carbon via fusion of three alpha particles in red giant stars. In this Letter, we present *ab initio* lattice calculations which unravel the structure of the Hoyle state, along with evidence for a low-lying spin-2 rotational excitation. For the ^{12}C ground state and the first excited spin-2 state, we find a compact triangular configuration of alpha clusters. For the Hoyle state and the second excited spin-2 state, we find a "bent-arm" or obtuse triangular configuration of alpha clusters. We also calculate the electromagnetic transition rates between the low-lying states of ^{12}C.

The carbon nucleus ^{12}C is produced by fusion of three alpha particles in red giant stars. However, without resonant enhancement the triple alpha reaction is too slow to account for the observed abundance of carbon in the Universe. In the early 1950s, Öpik and Salpeter noted independently that the first step of merging two alpha particles is enhanced by the formation of ^{8}Be [1–3]. The ground state of ^{8}Be is a resonance with energy 92 keV above the ^{4}He-^{4}He threshold and a width of 2.5 eV. However, a year later Hoyle realized that this enhancement is still insufficient. To resolve this discrepancy, Hoyle predicted an unobserved positive-parity resonance of ^{12}C just above the combined masses of ^{8}Be and ^{4}He [4].

About three years later, Cook, Fowler, Lauritsen, and Lauritsen observed a $J^\pi = 0^+$ state 278 keV above the ^{8}Be-^{4}He threshold [5]. This excited 0_2^+ state has a width of 8.5 eV, and is now commonly known as the "Hoyle state." The triple alpha reaction is completed when the Hoyle state decays electromagnetically to the 2_1^+ state and, subsequently, to the 0_1^+ ground state. Around the same time, Morinaga conjectured that the structure of excited alpha-nuclei such as the Hoyle state may be nonspherical [6], which would imply low-lying rotational excitations of even parity. Other ideas also exist for the structure of the Hoyle state, such as a diffuse trimer of alpha particles [7]. Recently, the spin-2 excitation of the Hoyle state has attracted considerable interest from several experimental groups [8–12].

We have recently presented an *ab initio* lattice calculation of the Hoyle state [13] where the low-lying spectrum of ^{12}C was explored using the framework of chiral effective field theory and Monte Carlo lattice calculations. However the central question regarding the alpha cluster structure

of the Hoyle state remained unsolved, perhaps the greatest remaining challenge in *ab initio* nuclear theory. In this Letter, we announce a major innovation of the lattice method that constructs and tests a wide class of nuclear wave functions explicitly. We present *ab initio* lattice results that resolve questions about the structure of the Hoyle state and the existence of rotational excitations. We also find evidence for a low-lying spin-2 rotational excitation of the Hoyle state. For the Hoyle state and its spin-2 excitation, we find strong overlap with a "bent-arm" or obtuse triangular configuration of alpha clusters. This is in contrast with the ^{12}C ground state and the first spin-2 state, where we note strong overlap with a compact triangular configuration of alpha clusters. We also calculate the electromagnetic transition rates among the low-lying even-parity states of ^{12}C. Our lattice results can be compared with other recent theoretical calculations for the low-lying spectrum of ^{12}C using the no-core shell model [14,15] and variational calculations using Fermionic molecular dynamics [16,17].

Chiral effective field theory treats the interactions of protons and neutrons as a systematic expansion in powers of nucleon momenta and the pion mass. A recent review can be found in Ref. [18]. The low-energy expansion is organized in powers of Q, where Q denotes the typical particle momentum and is treated on the same footing as the mass of the pion. The most important contributions to the nuclear Hamiltonian appear at leading order (LO) or $\mathcal{O}(Q^0)$, while the next-to-leading order (NLO) terms are $\mathcal{O}(Q^2)$. In the lattice calculations presented here, we include all possible interactions up to next-to-next-to-leading order (NNLO), or $\mathcal{O}(Q^3)$.

Our analysis makes use of a periodic cubic lattice with a lattice spacing of $a = 1.97$ fm and a length of $L = 12$ fm. In the time direction, we use a step size of $a_t = 1.32$ fm and vary the propagation time L_t to extrapolate to the limit $L_t \rightarrow \infty$. The nucleons are treated as pointlike particles on lattice sites, and interactions due to the exchange of pions and multi-nucleon operators are generated using auxiliary fields. Lattice effective field theory was originally used to calculate the many-body properties of homogeneous nuclear and neutron matter [19,20]. Since then, the properties of several atomic nuclei have been investigated [21,22]. A recent review of the literature can be found in Ref. [23].

We use Euclidean time propagation to project on to low-energy states of the interacting system. Let H be the Hamiltonian. For any initial quantum state Ψ, the projection amplitude is defined as the expectation value $\langle e^{-Ht} \rangle_\Psi$. For large Euclidean time t, the exponential operator e^{-Ht} enhances the signal of low-energy states. Energies can then be determined from the exponential decay of these amplitudes. The first and last few time steps are evaluated using a simpler Hamiltonian $H_{\text{SU(4)}}$, based upon the Wigner SU(4) symmetry for protons and neutrons [24]. Such a Hamiltonian is computationally inexpensive and is used as a low-energy filter before the main calculation. This technique is described in Ref. [23].

In Table I, we present lattice results for the ground state energies of ^{4}He and ^{8}Be up to NNLO. The method of calculation is nearly identical to that described in Refs. [13,22,25]. As discussed in these references, our LO result already includes a large portion of the corrections usually counted at NLO. Therefore the scaling of corrections with increasing order decreases much more rapidly than suggested by the results in Table I. The higher-order corrections are computed using perturbation theory, and the coefficients of the nucleon-nucleon interaction are determined by fitting available low-energy scattering data. In our calculations the NNLO corrections correspond to three-nucleon forces. A detailed description of the interactions at each order can be found in Ref. [25]. We have used the triton binding energy and the weak axial vector current to fix the low-energy constants c_D and c_E which enter the three-nucleon interaction. In comparison with Ref. [13], improvements have been made using

higher-derivative lattice operators which eliminate the overbinding of the LO action for larger nuclei such as ^{16}O. The details of this improved action will be discussed in a forthcoming publication. We note that the computed binding energies for ^{4}He and ^{8}Be at NNLO are in agreement with the experimental values.

In our projection Monte Carlo calculations, we use a larger class of initial and final states than hitherto considered. For ^{4}He, we use an initial state with four nucleons, each at zero momentum. For ^{8}Be, we use the same initial state as for ^{4}He, followed by application of creation operators after the first Euclidean time step in order to inject four more nucleons at zero momentum. An analogous procedure is performed in order to extract four nucleons before the last Euclidean time step. Such injection and extraction of nucleons at zero momentum helps to eliminate directional biases caused by the initial and final state momenta.

We make use of many different initial and final states in order to probe the structure of the various ^{12}C states. For the ^{12}C states investigated here, we measure four-nucleon correlations by calculating the expectation value $\langle \rho^4 \rangle$, where ρ is the total nucleon density. We find strong four-nucleon correlations consistent with the formation of alpha clusters. In Fig. 1, we present lattice results for the energy of ^{12}C at leading order versus Euclidean projection time t. For each of the initial states $A - D$, we start with delocalized nucleon standing waves and use a strong attractive interaction in $H_{\text{SU(4)}}$ to allow the nucleons to self-organize into a nucleus. For the initial states Δ and Λ, we use alpha cluster wave functions to recover the same states found using the initial states $A - D$. For these calculations, the interaction in $H_{\text{SU(4)}}$ is not as strong and the projected states retain their original alpha cluster character.

In Panel I of Fig. 1, we show lattice results corresponding to the initial states A, B, and Δ, each approaching the ground state energy $-96(2)$ MeV. For initial state A, we start with four nucleons (each at zero momentum) apply
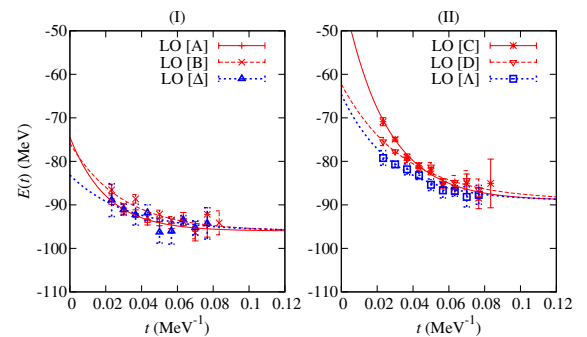
TABLE I. Lattice results and experimental values for the ground state energies of ^{4}He and ^{8}Be, in units of MeV. The quoted errors are one standard deviation estimates which include both Monte Carlo statistical errors and uncertainties due to extrapolation at large Euclidean time.

	^{4}He	^{8}Be
LO [$\mathcal{O}(Q^0)$]	$-28.0(3)$	$-57(2)$
NLO [$\mathcal{O}(Q^2)$]	$-24.9(5)$	$-47(2)$
NNLO [$\mathcal{O}(Q^3)$]	$-28.3(6)$	$-55(2)$
Expt.	-28.30	-56.50

FIG. 1 (color online). Lattice results for the ^{12}C spectrum at leading order (LO). Panel I shows the results using initial states A, B, and Δ, each of which approaches the ground state energy. Panel II shows the results using initial states C, D, and Λ. These trace out an intermediate plateau at an energy $\simeq 7$ MeV above the ground state.
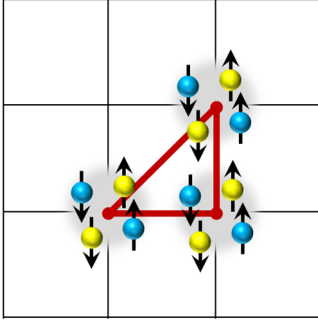
FIG. 2 (color online).   Illustration of the initial state Δ. There are 12 equivalent orientations of this compact triangular configuration.

creation operators after the first time step to inject four more nucleons at rest, followed by the injection of four additional nucleons at rest after the second time step. This procedure is used in reverse to extract nucleons for the final state A. An identical scheme is used for initial state B, though the interactions in $H_{\mathrm{SU(4)}}$ are not as strongly attractive as those for A.

For the initial state Δ, we use a wave function constructed from of three alpha clusters, as shown in Fig. 2. The alpha clusters are formed by Gaussian wave packets centered on the vertices of a compact triangle. In order to construct eigenstates of total momentum and lattice cubic rotations, we consider all possible translations and rotations of the initial state. There are a total of 12 equivalent orientations of Δ. We do not find rapid convergence to the ground state when starting from any other configuration of alpha clusters. We thus conclude that the alpha cluster configurations in Fig. 2 have the strongest overlap with the 0_1^+ ground state of ^{12}C. The fact that Δ is an isosceles right triangle rather than an equilateral triangle is merely a lattice artifact.

In Panel II of Fig. 1, we show the leading-order energies obtained from the initial states C, D, and Λ. Each of these approaches an intermediate plateau at $-89(2)$ MeV. In the limit of infinite Euclidean time, these would eventually also approach the ground state energy. However, it is clear that a different state is first being formed which is distinct from the
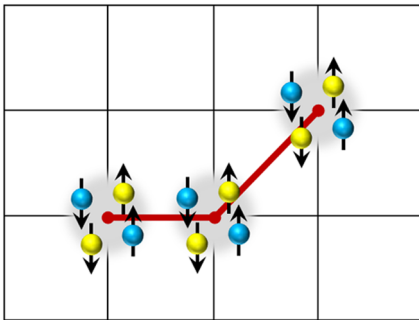

FIG. 3 (color online).   Illustration of the initial state Λ. There are 24 equivalent orientations of this bent-arm or obtuse triangular configuration.

ground state. We identify the 0^+ state in this plateau region as the 0_2^+ Hoyle state. The common thread connecting the initial states C, D, and Λ is that each produces a state which has an extended (or prolate) geometry. This is in contrast to the oblate triangular configuration shown in Fig. 2.

For initial state C, we take four nucleons at rest, four with momenta $(2\pi/L, 2\pi/L, 2\pi/L)$, and four with momenta $(-2\pi/L, -2\pi/L, -2\pi/L)$. Similarly, for initial state D we take four nucleons at rest, four with momenta $(2\pi/L, 2\pi/L, 0)$, and four with momenta $(-2\pi/L, -2\pi/L, 0)$. Finally, initial state Λ uses a set of three alpha clusters formed by Gaussian wave packets centered on the vertices of a bent-arm (or obtuse) triangular configuration, as shown in Fig. 3. There are a total of 24 equivalent orientations of Λ. We do not find the same energy plateau starting from other configurations of alpha clusters. We conclude that configurations of the type shown in Fig. 3 have the strongest overlap with the 0_2^+ Hoyle state of ^{12}C.

We use the multichannel method of Ref. [13] to find a spin-2 excitation above the ground state, as well as a spin-2 excitation above the Hoyle state. In both cases, we make use of the E^+ representation of the cubic rotation group on the lattice. We summarize our results for the binding energies of the low-lying, even-parity states of ^{12}C in Table II. The binding energies at NNLO are in agreement with the experimental values.

In Table III, we present results at LO for the root-mean-square charge radii and quadrupole moments of the even-parity states of ^{12}C, with experimental values given where available. In this study, we compute electromagnetic moments only at LO. We note that moments such as the charge radius for resonances above threshold are dependent

TABLE II.   Lattice and experimental results for the energies of the low-lying even-parity states of ^{12}C, in units of MeV.

	0_1^+	$2_1^+(E^+)$	0_2^+	$2_2^+(E^+)$
LO	$-96(2)$	$-94(2)$	$-89(2)$	$-88(2)$
NLO	$-77(3)$	$-74(3)$	$-72(3)$	$-70(3)$
NNLO	$-92(3)$	$-89(3)$	$-85(3)$	$-83(3)$
Expt.	-92.16	-87.72	-84.51	$-82.6(1)$ [8,10]
				$-81.1(3)$ [9]
				$-82.32(6)$ [11]

TABLE III.   Lattice results at leading order (LO) and experimental values for the root-mean-square charge radii and quadrupole moments of the ^{12}C states.

	LO	Expt.
$r(0_1^+)$ [fm]	2.2(2)	2.47(2) [26]
$r(2_1^+)$ [fm]	2.2(2)	$\cdots$
$Q(2_1^+)$ [$e\,\mathrm{fm}^2$]	6(2)	6(3) [27]
$r(0_2^+)$ [fm]	2.4(2)	$\cdots$
$r(2_2^+)$ [fm]	2.4(2)	$\cdots$
$Q(2_2^+)$ [$e\,\mathrm{fm}^2$]	$-7(2)$	$\cdots$

TABLE IV.   Lattice results at leading order (LO) and experimental values for electromagnetic transitions involving the even-parity states of ^{12}C.

	LO	Expt.
$B(E2, 2_1^+ \rightarrow 0_1^+)$ $[e^2\,\mathrm{fm}^4]$	5(2)	7.6(4) [28]
$B(E2, 2_1^+ \rightarrow 0_2^+)$ $[e^2\,\mathrm{fm}^4]$	1.5(7)	2.6(4) [28]
$B(E2, 2_2^+ \rightarrow 0_1^+)$ $[e^2\,\mathrm{fm}^4]$	2(1)	...
$B(E2, 2_2^+ \rightarrow 0_2^+)$ $[e^2\,\mathrm{fm}^4]$	6(2)	...
$m(E0, 0_2^+ \rightarrow 0_1^+)$ $[e\,\mathrm{fm}^2]$	3(1)	5.5(1) [17]

on the boundary conditions used to regulate the continuum-state asymptotics of the wave function. We avoid this problem, because all of the low-lying states are bound at LO. One expects that as the higher-order corrections push the binding energies closer to the triple alpha threshold, the corresponding radii will increase accordingly. A detailed study of these resonances as a function of lattice volume will be undertaken in future work. We find good agreement with the experimental value for the 2_1^+ quadrupole moment. The sign difference of the electric quadrupole moments of the spin-2 states is a reflection of the oblate shape of the 2_1^+ state and the prolate shape of the 2_2^+ state.

The LO results for the electromagnetic transitions among the even-parity states of ^{12}C are shown in Table IV. For a definition of the quantities shown, see, e.g., Ref. [29]. We find reasonable agreement with available experimental data. The lattice results at LO have a tendency to slightly underestimate the experimental values. Presumably, this reflects the greater binding energies and smaller radii of the nuclei at LO. We also predict electromagnetic decays involving the 2_2^+ state, which are likely to be measured experimentally in the near future.

In summary, we have presented *ab initio* lattice calculations which reveal the structure of the Hoyle state and find evidence for a low-lying spin-2 rotational excitation. For the ground state and the first spin-2 state, we find mostly a compact triangular configuration of alpha clusters. For the Hoyle state and the second spin-2 state, we find a bent-arm or obtuse triangular configuration of alpha clusters. We have calculated charge radii, quadrupole moments and electromagnetic transitions among the low-lying even-parity states of ^{12}C at LO. All of our results are in reasonable agreement with experiment. While further work is clearly needed (such as calculations using smaller lattice spacings), our results provide a deeper understanding starting from first principles, of the structure and rotations of the Hoyle state.

[1] E. J. Öpik, Proc. R. Irish Acad., Sect. A **54**, 49 (1951).
[2] E. E. Salpeter, Astrophys. J. **115**, 326 (1952).
[3] E. E. Salpeter, Annu. Rev. Nucl. Sci. **2**, 41 (1953).
[4] F. Hoyle, Astrophys. J. Suppl. Ser. **1**, 121 (1954).
[5] C. Cook, W. A. Fowler, C. C. Lauritsen, and T. Lauritsen, Phys. Rev. **107**, 508 (1957).
[6] H. Morinaga, Phys. Rev. **101**, 254 (1956).
[7] A. Tohsaki, H. Horiuchi, P. Schuck, and G. Röpke, Phys. Rev. Lett. **87**, 192501 (2001).
[8] M. Freer *et al.*, Phys. Rev. C **80**, 041303 (2009).
[9] S. Hyldegaard *et al.*, Phys. Rev. C **81**, 024303 (2010).
[10] W. R. Zimmerman, N. E. Destefano, M. Freer, M. Gai, and F. D. Smit, Phys. Rev. C **84**, 027304 (2011).
[11] M. Itoh *et al.*, Phys. Rev. C **84**, 054308 (2011).
[12] F. Smit *et al.*, Phys. Rev. C **86**, 037301 (2012).
[13] E. Epelbaum, H. Krebs, D. Lee, and U.-G. Meißner, Phys. Rev. Lett. **106**, 192501 (2011).
[14] R. Roth, J. Langhammer, A. Calci, S. Binder, and P. Navratil, Phys. Rev. Lett. **107**, 072501 (2011).
[15] C. Forssen, R. Roth, and P. Navratil, arXiv:1110.0634.
[16] M. Chernykh, H. Feldmeier, T. Neff, P. von Neumann-Cosel, and A. Richter, Phys. Rev. Lett. **98**, 032501 (2007).
[17] M. Chernykh, H. Feldmeier, T. Neff, P. von Neumann-Cosel, and A. Richter, Phys. Rev. Lett. **105**, 022501 (2010).
[18] E. Epelbaum, H.-W. Hammer, and U.-G. Meißner, Rev. Mod. Phys. **81**, 1773 (2009).
[19] H. M. Müller, S. E. Koonin, R. Seki, and U. van Kolck, Phys. Rev. C **61**, 044320 (2000).
[20] D. Lee, B. Borasoy, and T. Schäfer, Phys. Rev. C **70**, 014007 (2004).
[21] E. Epelbaum, H. Krebs, D. Lee, and U.-G. Meißner, Eur. Phys. J. A **41**, 125 (2009).
[22] E. Epelbaum, H. Krebs, D. Lee, and U.-G. Meißner, Phys. Rev. Lett. **104**, 142501 (2010).
[23] D. Lee, Prog. Part. Nucl. Phys. **63**, 117 (2009).
[24] E. Wigner, Phys. Rev. **51**, 106 (1937).
[25] E. Epelbaum, H. Krebs, D. Lee, and U.-G. Meißner, Eur. Phys. J. A **45**, 335 (2010).
[26] L. A. Schaller, L. Schellenberg, T. Q. Phan, G. Piller, A. Ruetschi, and H. Schneuwly, Nucl. Phys. **A379**, 523 (1982).
[27] W. J. Vermeer, M. T. Esat, J. A. Kuehner, R. H. Spear, A. M. Baxter, and S. Hinds, Phys. Lett. **122B**, 23 (1983).
[28] F. Ajzenberg-Selove, Nucl. Phys. **A506**, 1 (1990).
[29] A. Bohr and B. R. Mottelson, *Nuclear Structure. Single-Particle Motion* (W. A. Benjamin, New York, 1969), Vol. I.